# Research and Development for Continued Performance Improvement in Flexible a-Si PV

**Final Report on Contract No.** W911QY-10-C-0019

**Dates: 14 December 2009 to 14 December 2010**

Submitted by

Steven Braymen
PowerFilm, Inc.
2337 230th St
Ames, IA 50014

# REPORT DOCUMENTATION PAGE



PLEASE DO NOT RETURN YOUR FORM TO THE ABOVE ADDRESS.

| 1. REPORT DATE | 2. REPORT TYPE | 3. DATES COVERED |
|---|---|---|
| 12/14/2009-12/14/2010 | Final Technical Report | 12/14/2009-12/14/2010 |

**4. TITLE AND SUBTITLE**

Research and Development for Continued Performance Improvement in Flexible a-Si PV

**5a. CONTRACT NUMBER**

W911QY-10-C-0019

**5b. GRANT NUMBER**

**5c. PROGRAM ELEMENT NUMBER**

**6. AUTHOR(S)**

Steven Braymen

**5d. PROJECT NUMBER**

**5e. TASK NUMBER**

**5f. WORK UNIT NUMBER**

**7. PERFORMING ORGANIZATION NAME(S) AND ADDRESS(ES)**

Power Film Inc.
2337 230th St.
Ames, IA 50014

**8. PERFORMING ORGANIZATION REPORT NUMBER**

**9. SPONSORING/MONITORING AGENCY NAME(S) AND ADDRESS(ES)**

U.S. Army Soldier Systems Center – Natick
Attn: Steven Tucker
Kansas Street
Natick, MA 01760-5000
MARK FOR: W911QY-10-C-0019

**10. SPONSOR/MONITOR'S ACRONYM(S)**

**11. SPONSOR/MONITOR'S REPORT NUMBER(S)**

**12. DISTRIBUTION/AVAILABILITY STATEMENT**

unrestricted/unclassified

**13. SUPPLEMENTARY NOTES**

**14. ABSTRACT**

There are many aspects to power generation from an amorphous silicon tandem solar module as produced by Power Film Inc. These include the tunnel junction between the top and lower layer of the cell, the life time, as affected by the Staebler-Wronski effect, and the band gap of the photon collecting layers. The manufacturing process and source materials have a large impact on each of these areas. In this study, the tunnel junction was modified to act as a recombination junction in order to reduce the reverse voltage bias. The intrinsic silicon layers were modified to minimize the Staebler-Wronski effect. Additionally, carbon was added as a dopant to the top intrinsic silicon layer to boost over all cell performance by modifying the band gap of the material.

**15. SUBJECT TERMS**

life time, PV, photovoltaic, Staebler-Wronski, carbon doping, recombination, junction

| 16. SECURITY CLASSIFICATION OF: | | | 17. LIMITATION OF ABSTRACT | 18. NUMBER OF PAGES | 19a. NAME OF RESPONSIBLE PERSON |
|---|---|---|---|---|---|
| a. REPORT | b. ABSTRACT | c. THIS PAGE | | | Steven Braymen |
| U | U | U | UU | 39 | 19b. TELEPHONE NUMBER (515) 292-7606 x104 |

Standard Form 298

**Abstract**

There are many aspeets to power generation from an amorphous silicon tandem solar module as produced by Power Film Inc. These inelude the tunnel junction between the top and lower layer of the eell, the life time, as affeeted by the Staebler-Wronski effect, and the band gap of the photon eollecting layers. The manufacturing process and source materials have a large impaet on eaeh of these areas. In this study, the tunnel junetion was modified to aet as a reeombination junction in order to reduce the reverse voltage bias. The intrinsie silieon layers were modified to minimize the Staebler-Wronski effeet. Additionally, carbon was added as a dopant to the top intrinsie silieon layer to boost over all eell performanee by modifying the band gap of the material.

## Table of Contents

## List of Figures

Figure C.3.3 The index of refraction of the silieon-carbon films using different spectral minima, indieating the index as a funetion of wavelength of light for varying carbon content.
Figure C.3.4. The 3% and 6% data points have been added to a previously seen graph. The refraetive index continues the trend of higher index with less earbon.

Figure C.3.5 I-V curve of a carbon doped amorphous silieon solar cell.

Figure C.3.6 Measured parameters for earbon doped amorphous silicon solar cell.

Figure C.3.7 Sample 6 is 0% aeetylene and Sample 8 is 2.4% acetylene.

Figure C.3.8 Open circuit voltage, Voc, plotted against the Acetylene flow. Each sample measured is represented by a blue diamond on the graph; the average for each flow set point is displayed as a red square.

Figure C.3.9 Fill Faetor, ff, plotted against the Aeetylene flow.

Figure C.2.10 Maximum power point power, MPP, plotted against the Acetylene flow.
Figure C.3.11 Refractive index of carbon doped amorphous silicon as measured with ellipsometery. (0% is Power Film's standard material.)

Figure C.3.12 Extinction coefficient of carbon doped amorphous silicon as measured with ellipsometery. (0% is Power Film's standard material.)

Figure C.3.13 IV eurve test of PV modules with carbon doping. Note: the fill factor (FF) and power at max power point (Pmpp) are divided by a factor of 10 for displace purposes.

Figure C.3.14 The graph below shows the eleetrieal results for Voe, Isc, FF, and Pmpp. There trend is towards lower RF power or thinner layers of earbon doped 12.

Figure C.4.1 IV eurve representing the deliverable material

Table A.2.1 Comparison of various surface treatments.
A.4.1 Open eireuit voltage comparison for various surface treatments

Table A.2.2: Recombination layer deposition parameters

Table A.2.3 Recombination layer DC plasma deposition properties
Table C.3.1 Properties of carbon doped silieon films.

Table C.3.2 the natural log of the current (Ln(I)) versus reeiprocal temperature (1/T) is shown.

## Summary

This body of work was section into three parts. The first dealt with the addition of a recombination layer between the top and bottom layers of Power Film Inc.'s tandem cell amorphous silicon photovoltaic, PV, material. The second part dealt with improving the long term stability concerning the Staebler-Wronski effect. Finally, carbon doping was added to the top intrinsic layer in order to change the band gap of the material in order to allow more light to reach the bottom layer and to increase the cell voltage.

A tunnel junction is formed between a highly degenerate layer of P-type microcrystalline silicon and a highly degenerate layer of N-type microcrystalline silicon. The degeneracy allows for a near ohmic current path through the cell. However, being not completely ohmic resulting in a voltage loss. Adding a charger recombination layer at this junction would gain back this lost voltage. Introduction of a highly defective material would allow this to occur. In this work, many methods to incorporate a degenerate layer were attempted, including sputtering, chemical vapor deposition, and physical contact with a contaminated surface. In the end it was found that a contact to a surface provided the most consistent results.

The Staebler-Wronski effect is a well known problem for amorphous devices in that the fill factor declines up to 15% for tandem junctions and up to 30% for single junctions upon exposure to light. Its effect on PV device can be modified by the deposition parameters. Additionally, the lower intrinsic layer is effected more because it is thickest layer. In this work, the deposition parameters were modified and the effect by light degradation was studied. Many parameters were tested including temperature, deposition zone geometry, pressure, and hydrogen-silane dilution. Ultimately it was found that intrinsic layer film thickness and deposition temperature were the major players.

Carbon was incorporated into the top intrinsic layer to modify its properties. Acetylene was the carbon source of choice. Initially it was thought that the carbon addition would need to be significant, in the 10 to 20 % range. The carbon doped silicon was measured for a number of properties including refractive index and conductivity. It was found that for acetylene ratios greater then 2.5:40 the PV material performance was significantly degraded. The optimum ration was found to be 0.5:40. With carbon doping near the optimum it was found that PV power output increase 5%.

## Introduction

PowerFilm, (PF), a developer and manufacturer of flexible photovoltaics (PV) on plastic has been working for 8-9 years with Natick Soldier Research, Design and Engineering Center (NSRDEC) to develop and enhance PV for the military. During this time PowerFilm and NSRDEC have successfully developed a multitude of remote power solutions that have endured the rigors of evaluation by US military personnel in true field conditions. These items encompass a range of products from small lightweight foldable units to higher power PV integrated military shelters. PowerFilm and NSRDEC are continuing in their understanding of PV film manufacturing, leading to the development of real time monitoring methods and proprietary processes, resulting in improvement in overall devices and production costs. The primary factor in widespread adoption of any alternate energy source by the commercial market and, to some degree, the military has been the final cost. PowerFilm starts with manufacturing a very cost effective and unique thin film solar module on a polyimide (plastic) substrate. While moderate output per unit area (efficiency), these modules have the highest output per unit weight (specific power) of any available solar technology. Not only is the specific power is almost twice the next closest competitor and are also among the most durable. An advantage of this technology is that it can be further enhanced by improvements, which increases the output per unit area resulting in even higher specific power yields. These gains translate into smaller and lighter PV devices with more capabilities.

To this end, this research and development project was proposed to investigate the following opportunities for improvement.

**Recombination layer to improve device voltage**
The tunnel recombination junction is the junction between the top and bottom diodes in a tandem solar cell. Since PowerFilm fabricates "substrate" type solar cells, the tunnel-recombination junction will be deposited on top of the p-type layer of the bottom diode (P1) and will have the n-type layer of the top diode (N2) deposited on top of it, as shown in figure 1. Without a proper tunnel-recombination junction, the region between the P1 and N2 layers acts likes a reverse bias diode. This reverse bias diode creates a notch in the conduction and valence bands where both positive (+) and negative (-) charges accumulate and wait to recombine, as shown in figure 2a. Since the P1 and N2 layers are both microcrystalline silicon there are fewer traps than in amorphous silicon, so the charge carriers do not quickly and efficiently fall into traps and recombine. Accumulation of charge at the P1/N2 interface also means that an increased number of photons will be necessary to decrease the reverse bias on this interface. This leads to a reduction in the voltage output of the solar cell under a given light bias.

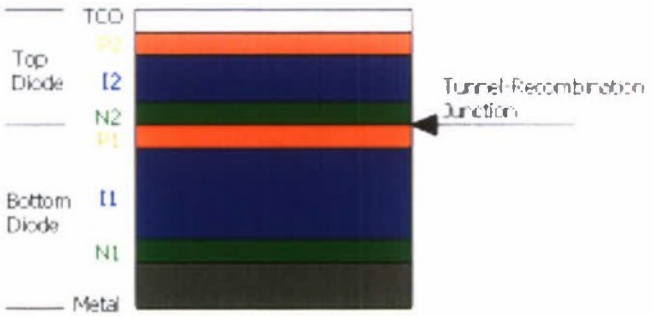


Figure 1: Diagram of solar material deposition stack.

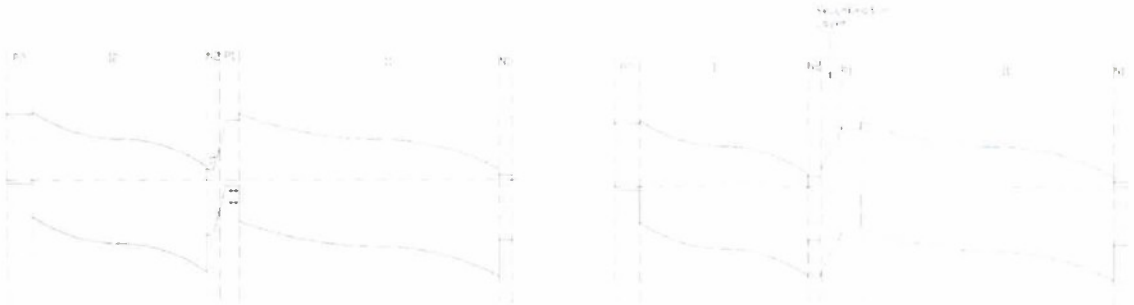

(a) (b)

Figure 2: Equilibrium band diagrams of solar cells (a) with and (b) without a tunnel recombination junction.

PowerFilm, Inc. conducted an in-depth study of various recombination layers and how they can be effieiently integrated into the deposition proeess. There are a number of different matcrials that could potentially be used to create a recombination layer. A few of these matcrials are: titanium nitride deposited by sputtering, titanium dcposited by sputtering, ehromium deposited by sputtering, silicon oxide deposited by plasma enhaneed chemical vapor deposition (PECVD), silieon nitride deposited by PECVD, intrinsie or doped zine oxide deposited by sputtering or low pressure chemieal vapor deposition, and intrinsie or dopcd amorphous silieon deposited by PECVD or hot wire chemieal vapor deposition. This projeet initially determined the materials, thicknesses, and deposition parameters that produee reeombination layers that yielded the largest inerease in module voltage and maximum output power at the modules power point. The results of this projeet was integrated into PowerFilm's eurrent process equipment.

Introduction of a reeombination layer has the potential to boost conversion efficiency of the solar modules by 10%. This increase in efficiency could potentially make PowerFilm's solar teehnology appealing to additional markets.

**Long term stability work**

Stability is a major coneern when producing any solar eells. Stability studies arc needed any time a change is made in the process, like that proposed above, to insure that no instability issues are introdueed. There is also the ongoing need of finding ways to improve stability.

The Staebler-Wronski effect is a well known effect in amorphous silicon that increases the number of states within the bandgap of the amorphous silicon upon illumination with light. Increases in gap states cause the fill factor of the solar cells to decrease. Geometry of the deposition system can have a major impact on the deposited material's quality. Currently, PowerFilm utilizes a plasma enhance chemical vapor deposition technique with parallel plate electrodes to deposit each of the amorphous and microcrystalline silicon layers within the solar cells.

While searching for ways to decrease the light induced degradation in the intrinsic amorphous silicon layers, the literature discussed the effects of electrode distance and temperature on the light induced degradation. A diagram of a parallel plate plasma enhance chemical vapor deposition, CVD, system is shown in Figure 3. In this case, it is believed that light induced degradation is reduced due to the suppression of higher order silane reactive species in the plasma, such as $S_2H_6$ and $S_3H_8$.

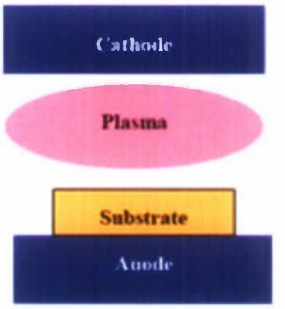


Figure 3. Block diagram of a CVD system

Increases in the stability of the amorphous silicon layers within PowerFilm's solar cells will increase the performance of the sold solar modules. Currently modules are sold at a much lower performance level than their actual initially tested performance, so that when light induced degradation takes place they will still meet the sold specification. Increased stability of the cells would increase the performance level that the solar modules could be sold at making PowerFilm's modules applicable in more markets. This will increase demand and cause PowerFilm to hire more employees in all areas of the company.

**Carbon doping of amorphous silicon for photovoltaic cells**

Our current tandem devices have a single cell output of about 1.7 volts. These individual cells are monolithically integrated, on the plastic substrate, in series to build voltages to desired levels. By adding carbon as a dopant into the a-Si, the voltage output of the PV material can be increased. This comes about because the carbon acts to increase the band gap of the a-Si material. Amorphous silicon has a band gap of approximately 1.8eV and it is believed that by adding carbon, this gap can be increased to greater then 2.0eV giving a boost to the module's output voltage. Use of the higher band gap material in the top junction of the tandem PV stack, leading to higher voltage, essentially allows a greater portion of the energy contained in the higher energy light, i.e. blue, to be utilized.

Carbon can be incorporated into the a-Si material by adding small concentrations of organic compounds to the PECVD deposition zone. Just as the silane breaks down, in the plasma, depositing silicon, and organic compounds can breakdown into carbon. PowerFilm Solar, Inc. proposes to use acetylene as the carbon source for doping the a-Si films. This new material will be incorporated into a heterojunction PV device as a carbon doped intrinsic silicon carrier generating layer with microcrystalline N and P layers for charge separation.

Power Film has evaluated the effect of this material on the PV performance as a function of carbon reactant concentration or flow rate.

## Technical Report:

## A. Study recombination layer effect

### A.1) Identify and test options for recombination layer and rank effectiveness in improving Voc

PowerFilm Solar, Inc. identified a few options to deposit a highly defective recombination layer between the top and bottom layer of the tandem PV device. These include hot wire, hot rod, glow discharge, sputter deposition and front roller.

### A.2) Evaluate options for depositing various layers and rank for suitability for inclusion in the Si deposition machines

**Hot Wire**

A deposition zone for performing hot-wires chemical vapor deposition experiments was fabricated as shown in Figure A.2.1. This design has a heated wire filament arranged in a U-shaped path, suspended across eight posts. The top of the zone is slotted to allow a directed deposition. This arrangement allows the reactant gases to be directed in through both ends and past a heated element, wire or rod etc., maintaining an even gas distribution.

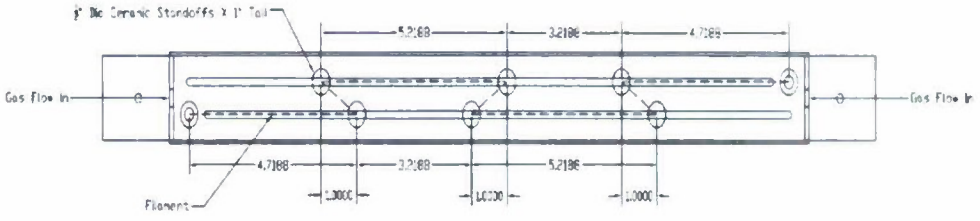


Figure A.2.1 Initial hot-wire box configuration.

This assembly was installed in one of PowerFilm's photovoltaic, PV, tandem device silicon machines so that it would deposit on the web between the lower and upper tandem layers.

Static depositions were made to test for functionality and uniformity. These depositions showed thicker deposition extending from the edge of the web, one to four inches from each side as shown in Figure A.1.2. This deposition appeared to occur close to the outside set of posts. This believed to be due to the fact that the silane was entering the box from the sides and was reacted on by the filament at the ends first, leaving less silane to be decomposed in the center of the filament. The uniformity for a static deposition using 9 seem of silane with no hydrogen is shown in Figure A.1.3. The uniformity for a static deposition using 130 sccm of silane and 1000 sccm of hydrogen is shown in Figure A.1.4. The hydrogen was added to act as a diluent for the silane and to increase the gas velocity through the hot wire box. Increasing both the amount of silane and the hydrogen improved the deposition uniformity, but it was still deemed not acceptable. Filament sag did not appear to be a problem with this configuration. The temperature of the web was controlled by a heated platen set to 187C. The filament was driven with a DC current of 10.6A

Figure A.2.2 Static deposition from initial hot-wire box.

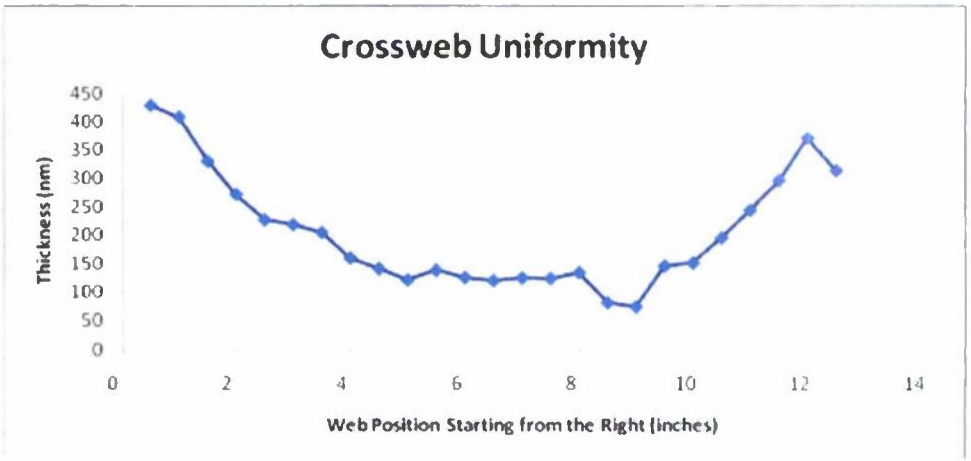


Figure A.2.3 Hot-wire deposition using 9 sccm of silane.

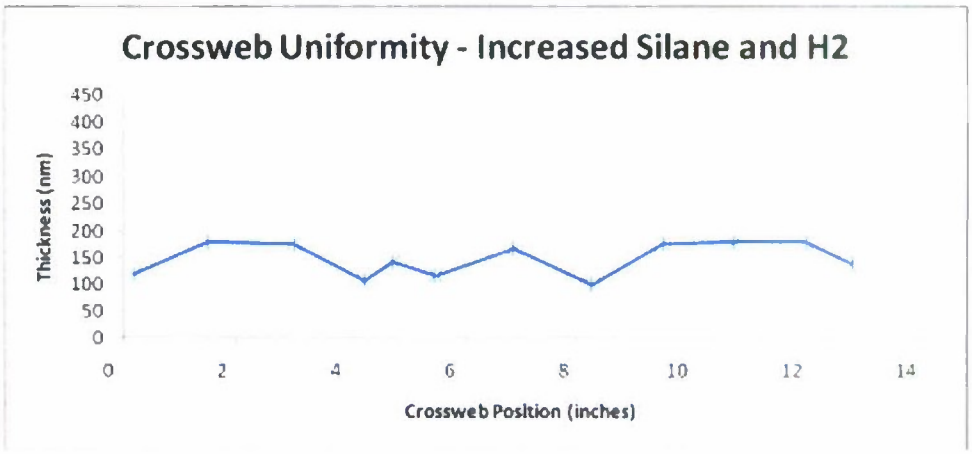


Figure A.2.4 Hot-wire deposition using 130 sccm of silane.

Non uniformity of the recombination layer remained a problem. To improve this uniformity, a gas shower head was added to the box to dispense the gas across the length of the filament instead of just on the two sides. A schematic of this new system is shown in Figure A.1.5 The shower head is shown in red and the filament is the dashed line.

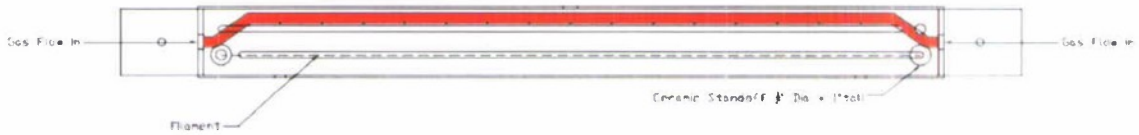


Figure A.2.5 Hot-wire zone with shower head installed.

Adding the shower head produced deposition that was thin in the center and thick on the edges, similar to earlier work. After examining the deposition and the deposition zone, it was determined that the non-uniformity was caused by filament sagging away from the web, leaving the deposition in the center to be much thinner than the edges. Based on thermal coefficient of thermal expansion, CTE, the amount of sag was estimated at about one inch.

Figure A.2.6 and A.2.7 shows the thickness of the deposited silicon for the right, left, and center of the web with various silane flow rates for static and moving depositions respectively.

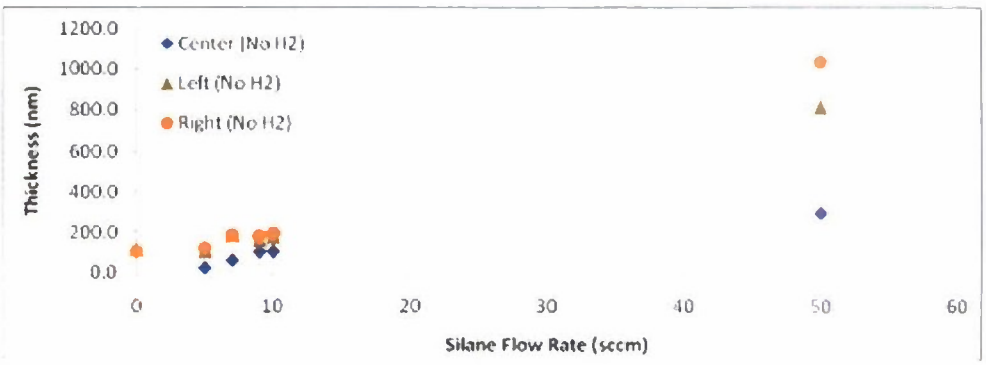

Figure A.2.6 Thickness of 10 minute statics for various silane flow rates.

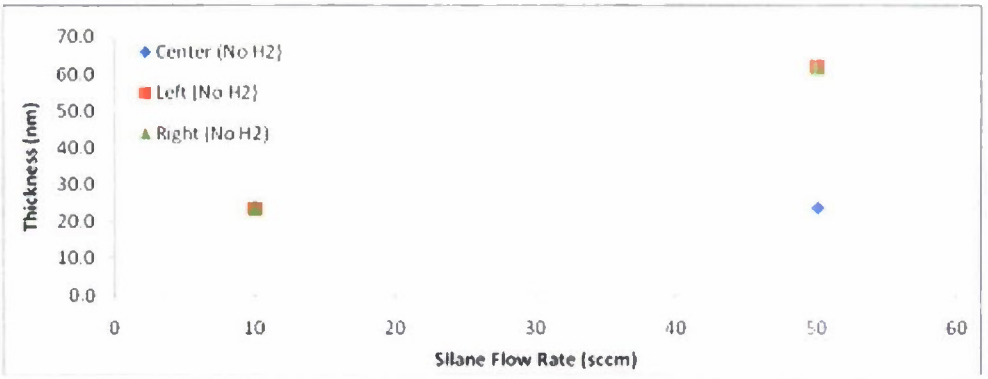


Figure A.2.7 Thickness of moving deposition (3"/min) for various silane flow rates.

New standoffs were designed to support the filament from sagging were tested.

Figure A.2.8 shows one example of how the filament compensated for the thermal expansion by creating a sinusoidal pattern. Figure A.1.9 shows a thicker and thinner deposition due to filament expansion for this standoff configuration.

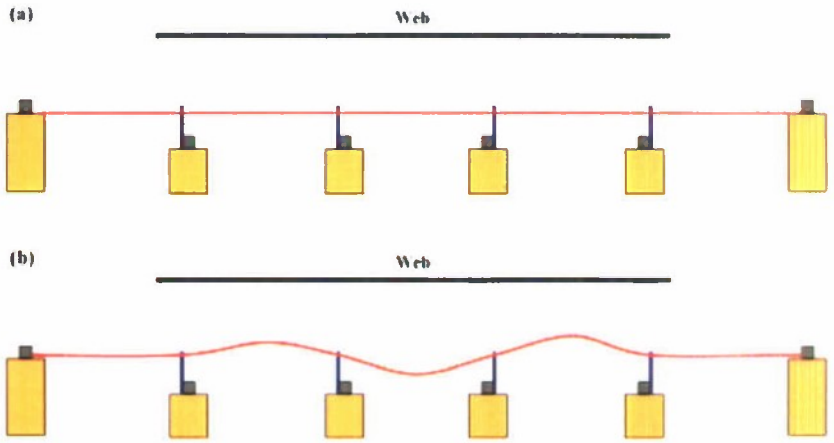


Figure A.2.8 Six evenly spaced standoffs support the filament below the web. (a) Before heating, the filament is in tension. (b) After heating, the filament expands and forces the filament to web distance to increase or decrease between pairs of standoffs.

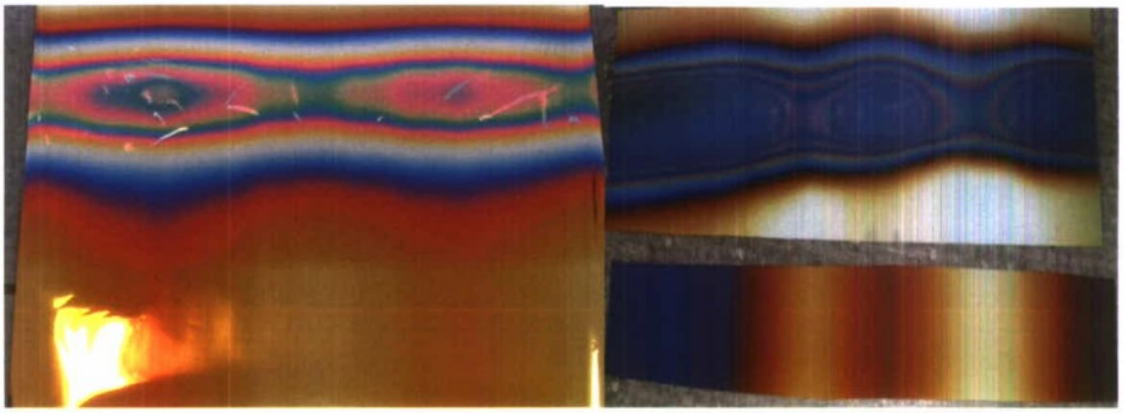

(a) (b)

Figure A.2.9 Statie depositions on top and moving depositions on the bottom for filaments supported by the standoff in Figure A.2.8.

Additionally alternating current, AC and direct current, DC, were used. It was determined that both AC current and DC current would yield the same deposition profiles and suggested that the AC power supply provide the necessary current in a more controllable manner.

To remedy the filament expansion problem various methods were tested. These were tension to the filament were using a coiled spring, using a counter weight, using a constant force spring (like a tape measure), or connecting one end of a wire to a rotary feed through and the other to a shaft with the filament connected.

High spring tension on the filament was between 4 and 4.5lbs, resulted in the filament breaking. The filament did not break with the tension set to 2 lbs. and also did not have any appreciable sagging. The statie deposition showed slightly more deposition from the edge of the web to about ½" in and a 6% thickness oscillation in the cross web direction due to ripples in the web, since the web was not riding on a platen above the hot-wire, as shown in Figure A.1.10. The deposition was performed with a filament current of 10.6A and using only the residual gases inside of the chamber from the plasma boxes. The plasmas were operating during this deposition. This type of deposition uniformity may be acceptable. To estimate the thickness for a deposition moving at 3 in/min the down-web thickness profile of the static was measured and is shown in Figure A.1.11. This thickness profile was integrated to estimate the total amount of silicon deposited in 10 minutes to be ~280nm. This means that a deposition moving at about 3"/min would yield a thickness of ~9nm.

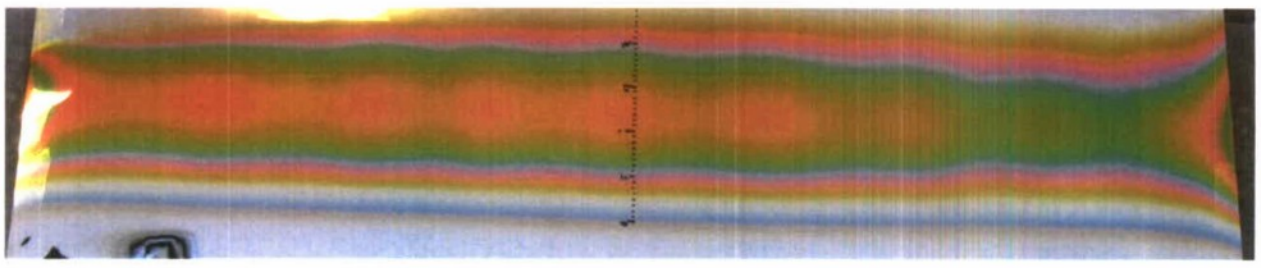

Figure A.2.10: Static deposition with the filament tensioned using a spring pulling on a linear stage on rails.

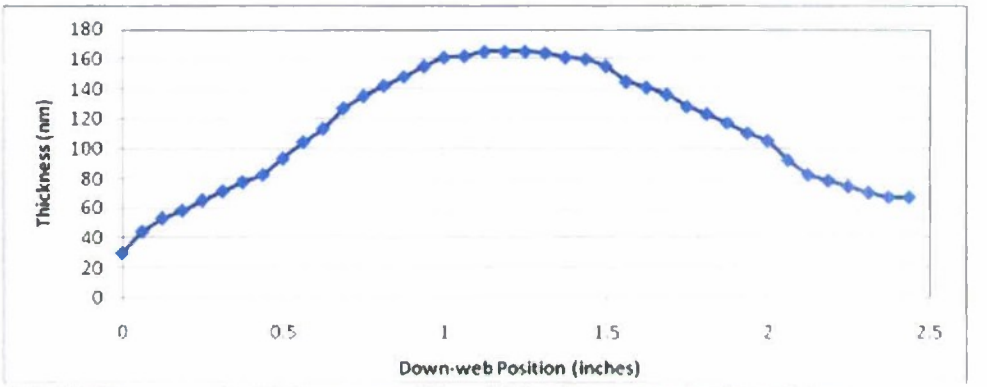


Figure A.2.11 Down-web thickness profile of 10 minute static deposition.

Tandem solar material was produced with a hot-wire tunnel-recombination layer between the bottom and top PV layers using filament temperatures. The results were ambiguous since multiple modules tested from a single condition with samples taken from different positions on the web showed significantly variation in performance. Figures A.2.12 and A.2.13 show the open circuit voltage and series resistance of the modules with respect to the current through the hot-wire filament. The scatter in the data is too large to discern a clear trend, however, it appears that the series resistance of the films containing a hot-wire tunnel-recombination layer are higher than those without.

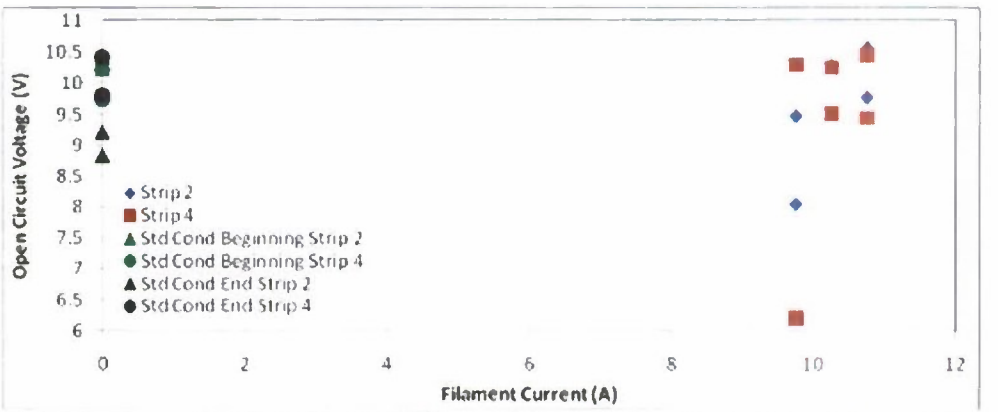


Figure A.2.12 Open circuit voltage of films with and without a hot-wire tunnel-recombination junction.

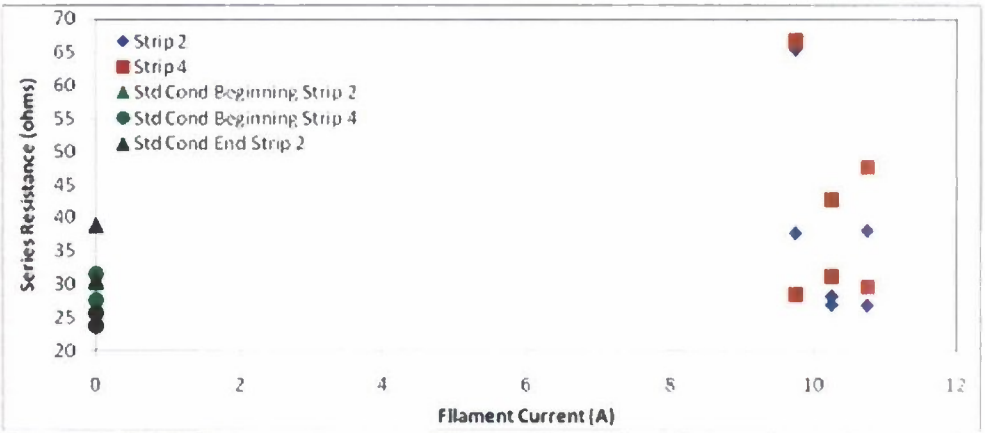

Figure A.2.13 Series resistance of films with and without a hot-wire tunnel-recombination junction.

The high series resistance of the solar modules, of the tunnel-recombination junction, with the hot wire deposition was determined to be too thick in all cases. To reduce the thickness of the deposition, operated the filament at a lower temperature, placing the filament farther from the web, and using a set of apertures were investigated.

Lowering the deposition temperature was easily accomplished, however, at low temperatures silicides tend to form on the surface of the filament, which affected filament lifetime and deposition rate and ultimately resulting in breaking for all trials.

A new hot-wire zone was designed and fabricated to address these issues. The new zone was designed with improvements to prevent non-uniformities due to the web curling etc. Ultimately, the choice became either one of non-uniformity due to too little filament tension allowing it to sag or to high of tension causing it to break.

**Hot Rod**

A 3.05 mm diameter graphite rod was substituted for the wire filament. Graphite was chosen as a material that it would not sag even when hot. After a quick test to determine applicable electric current requirements, a test was conducted using a graphite rod.

The rod driven with AC current at 45 amps produced enough heat to melt a 1/16" thick aluminum aperture and distorted the web, although it did not bend or sag. This test was repeated with current was stepped up from 20 to 40A in 5A increments, performing a 10 minute static deposition for each current level. In all cases, there was no deposition but there was still deformation of the web. The graphite rod used is the top rod shown in figure A.2.14.

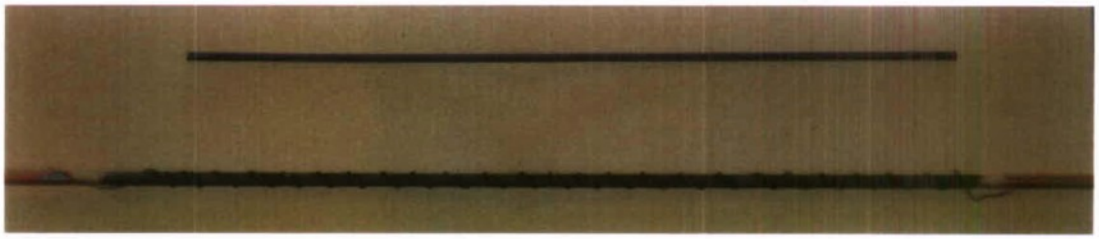

Figure A.2.14 (Top) Graphite rod used as a hot-wire. (Bottom) Tantalum filament wrapped around an alumina rod for support.

To reduce the heat generated, a tantalum filament wire was wrapped around a ¼" diameter alumina ceramic rod, as shown at the bottom of figure A.2.14. This system did deposit silicon on the web; however, the uniformity was poor and unpredictable because the silicon built up on the ceramic rod allowing some of the current to travel through the silicon instead of all of it going through the tantalum wire. These deposits created cold sections along the filament.

Because of the sagging and uniformity, options other then hot wire were considered.

**Titanium Nitride, sputtered**

As an alternative to the hot wire deposition of silicon, samples were prepared with various thicknesses of sputtered titanium nitride, TiN, as the recombination layer. This was intended to both improve the recombination and possibly reducing shunt paths.

A set of samples were produced using a 50 Angstrom TiN layer interstitial layer. These devices had good voltages, but the IV curve indicated severe shunting on one layer. At this point, it is uncertain whether the shunting is from particulate contamination on the web before the 2nd junction deposition or damage from sputtering the TiN.

Continuing with these tests, a significant increase in voltage was obtained with the sputtered TiN layer. As a comparison a sample which had the surface of the P-layer treated so that there was a thin layer of oxide formed, as an alternative to TiN as the recombination layer, was produced, however, it was shown to have no substantial effect, table A.2.1.

| Interface layer treatment | Voc | FF |
|---|---|---|
| None | 20.2 | 60 |
| Oxidation of P layer surface | 20.1 | 55 |
| 25 A of TiN | 22 | 60.5 |
| 50 A TiN | 21.8 | 56.9 |
| 100 A of TiN | 21.8 | 56 |

Table A.2.1 Comparison of various surface treatments.

It was found that a layer of TiN can be used as a recombination junction material. Thicker layers TiN does not improve voltage further, and can increase series resistance, lowering the Fill factor, (performance), of the device. This technique requires additional handling of the web with two addition processing steps. Reproducibility of this process was also poor.

**Glow Discharge**

As an alternative to hot-wire and TiN, a small plasma deposition zone was fabricated. This zone was essentially a small box with an antenna inside. This antenna was driven with a 4000V rectified 60 Hz AC power supply. Using a 2" x 16" antenna, a stabilized growth rate of 1.05nm/minute was achieved using the using residual process gases. With the antenna size reduced to 1" x 15.5" and a stabilized growth rate of 1.19nm/minute was achieved. The addition of 10sccm of SiH4 to the deposition zone averaged cross-web growth rates of 2.95nm/minute for the 2" wide antenna, and 4.50nm/minute for the 1" wide antenna.

By enclosing the antenna area fully except for the aperture, growth rate increased, using only residual process gases, to 3.54nm/minute.

The target film thickness is 5nm deposited in 3 minutes.

It is believed that the increase in rate using the smaller antenna and full glass enclosure may be occurring due to an increase in the power density at the antenna and in the aperture.

In all cases, for depositions performed using the ambient gases the cross-web uniformity was $\pm 3\%$. When additional silane was added to the deposition zone, the deposition became significantly thicker on the side of the box where the gas was entering. These thickness profiles are shown in figure A.2.15 and photo, figure A.2.16.

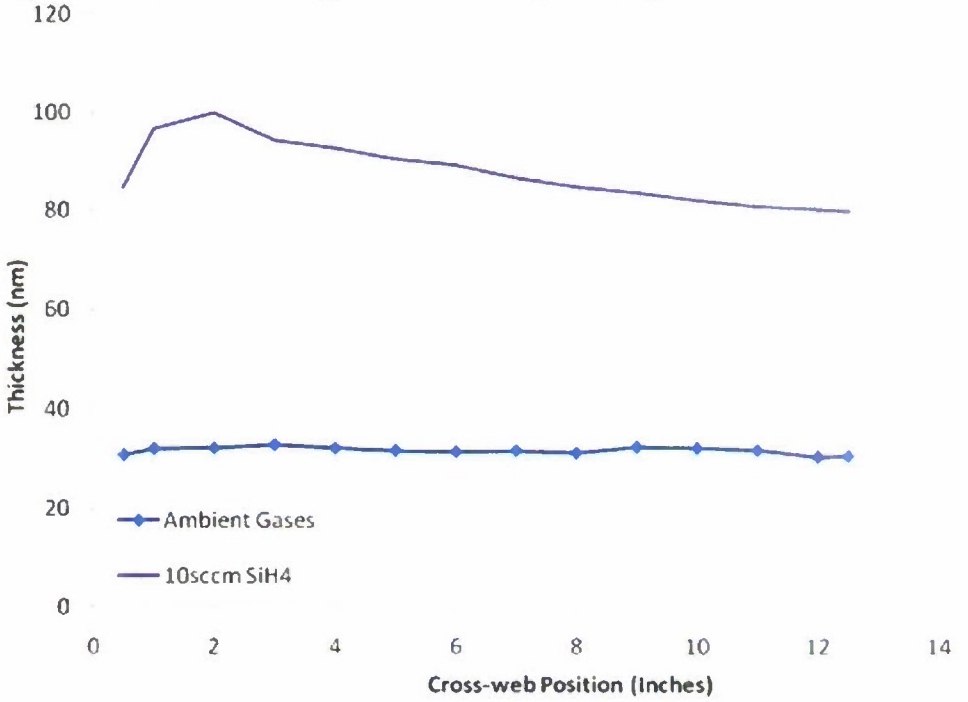


Figure A.2.15 Deposition thickness profiles for the plasma deposition zone, static, 10 minute each.


Figure A.2.16: Deposition using the plasma deposition zone with ambient gases.

To improve the uniformity of the layers deposited when additional gas was added to the deposition zone, gases were added from both sides of the deposition zone. Also, the spacing between the antenna and the web was inereased to about 5 1/8" putting the breakdown voltage at its minimum of 273V. This deereased the high voltage requirements from the power supply and allow for higher powers to be used. It was important to minimize the voltage in order to control arcing and damage to the apparatus and sample material.

Using the parameters listed in Table A.2.2, recombination material was deposited and sampled.

| Experimental Frame | Power (W) | Gas Flow |
|---|---|---|
| 0 | | Standard Tandem, No tunnel junetion |
| 1 | 102 | Ambient ehamber gas |
| 2 | 60 | Ambient chamber gas |
| 3 | 27 | Ambient chamber gas |
| 4 | 60 | 1 seem SiH4 |
| 5 | 64 | 1 seem SiH4, 1 seem B2H6 |
| 6 | | Standard Tandem, No tunnel junction |

Table A.2.2: Reeombination layer deposition parameters

It was found that there was no signifieant change in the open eireuit voltage of the devices for any of the deposition parameters used, as shown in Figure A.2.17. The performanee of the standard tandem material deposited at the beginning and end of the run had a great deal of seatter in the open eireuit voltages measured. Also, no speeific trend was apparent for samples with different tunnel junction deposition parameters, even when they were taken from the same region of the web in the eross-web direction. This indicates that the layer is probably too thin to create the required defect states allowing

recombination to occur and increase the open circuit voltage.

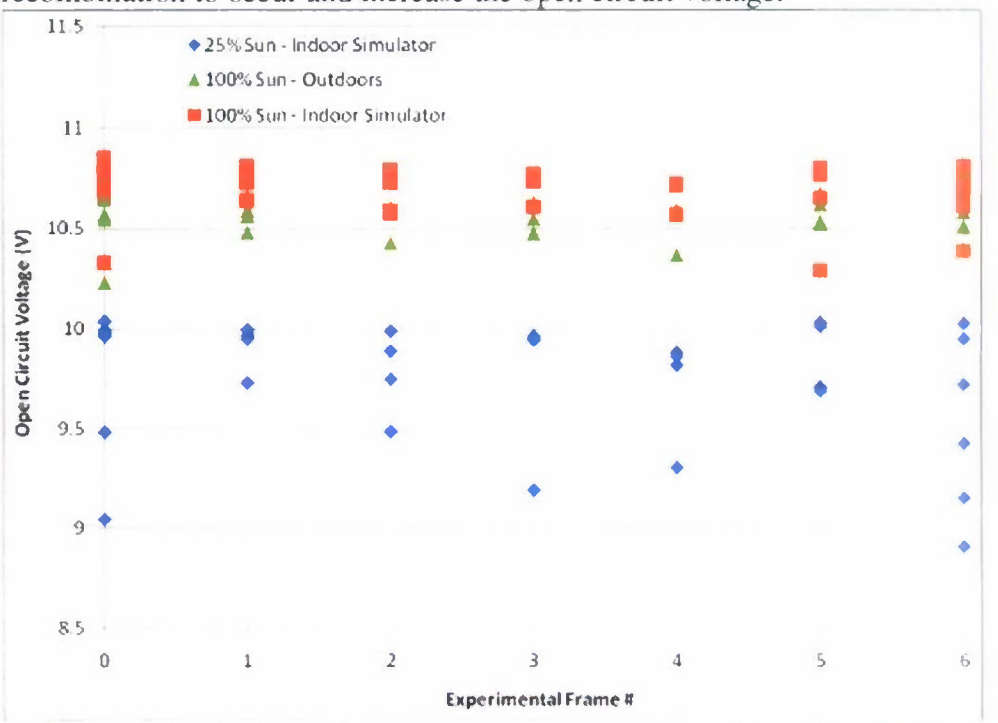


Figure A.2.17 Open circuit voltage measurements performed on each experimental frame.

From the results of carbon addition to the intrinsic layer, see section 'C', of the PV stack, the addition of acetylene can lead to a highly defective material. Since a highly defect material is considered being the preferred material for a recombination layer, the use of acetylene was investigated.

A series of recombination layers were deposited using a combination of silane and acetylene and the DC plasma deposition method. The combination of silane and acetylene has been shown to make very defect rich material, which is necessary for a good recombination layer. Table A.2.3 shows the parameters used for this set of experiments using C2H2 flow of 0.1 sccm and SiH4 flows of 0 to 20 sccm.

Recombination Layer Plasma Deposition Zone Parameters

| Experimental Frame | Voltage (V) | C2H2 Flow (sccm) | SiH4 Flow (sccm) |
|---|---|---|---|
| 0 | 0 | 0 | 0 |
| 1 | 2700 | 0.1 | 20 |
| 2 | 2700 | 0.1 | 5 |
| 3 | 2700 | 0.1 | 10 |
| 4 | 2700 | 0.1 | 1 |
| 5 | 2700 | 0.1 | 2 |

Table A.2.3 Recombination layer DC plasma deposition properties

In experimental frame 0 there was no plasma in the recombination layer deposition zone, so this is the control sample for the experiment. Experimental frames 1-5 were performed with varying silane flows with the acetylene flow held constant.

Figures A.2.18, .19, .20 and .21 show how the open circuit voltage, power point voltage, and power point power output changed with silane flow to the recombination layer deposition zone. Voltage and power increased initially and then decreased. This is probably due to a combination of an increasing deposited layer thickness and a decrease in defect states as silane flow increases. It is believed that the defect states are reduced as silane flow increases, due to the increase in the silane to acetylene ratio beyond a certain value.

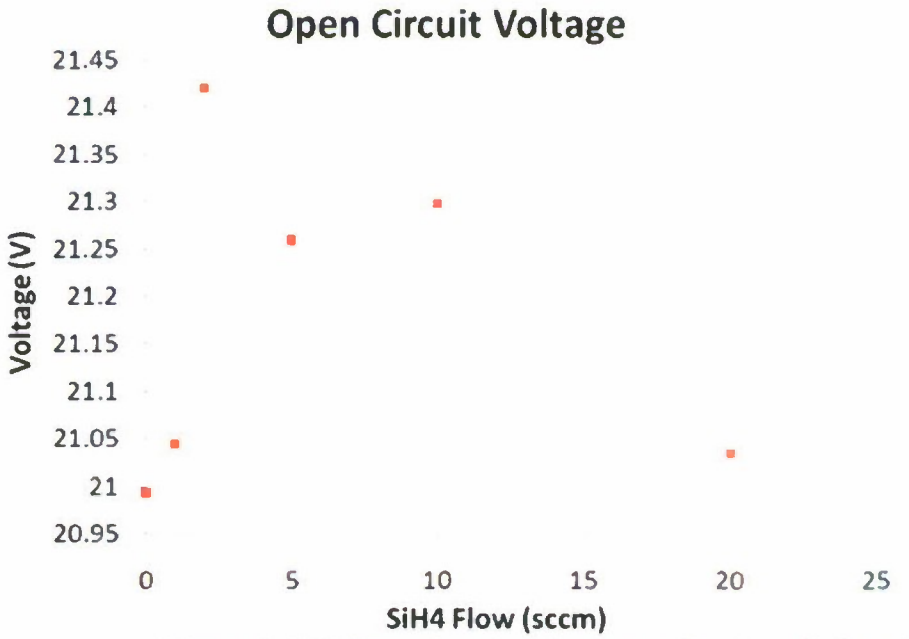


Figure A.2.18 Open circuit voltage as a function of silane flow with an acetylene flow of 0.1 sccm.

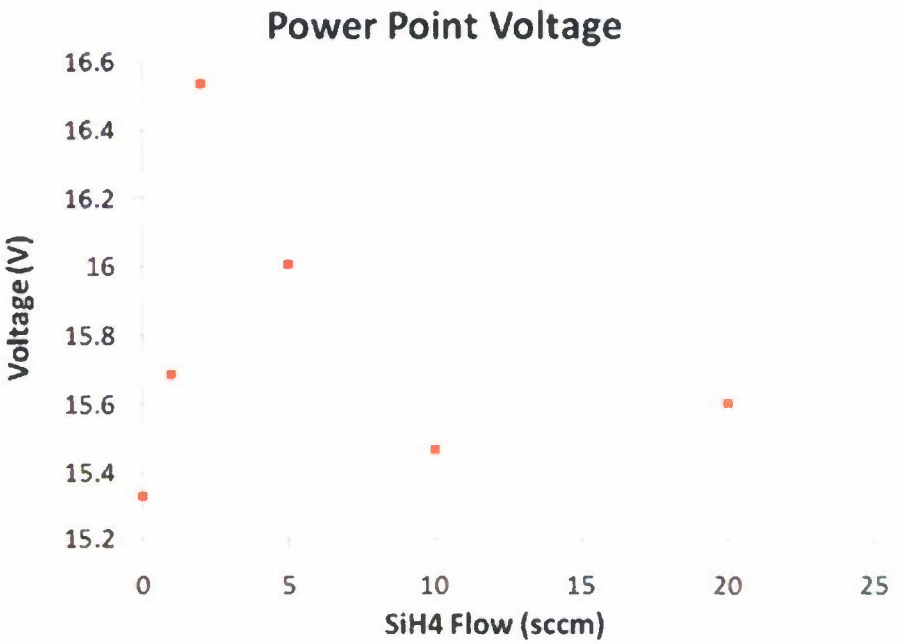


Figure A.2.19 Power Point voltage as a function of silane flow with an acetylene flow of 0.1 sccm.

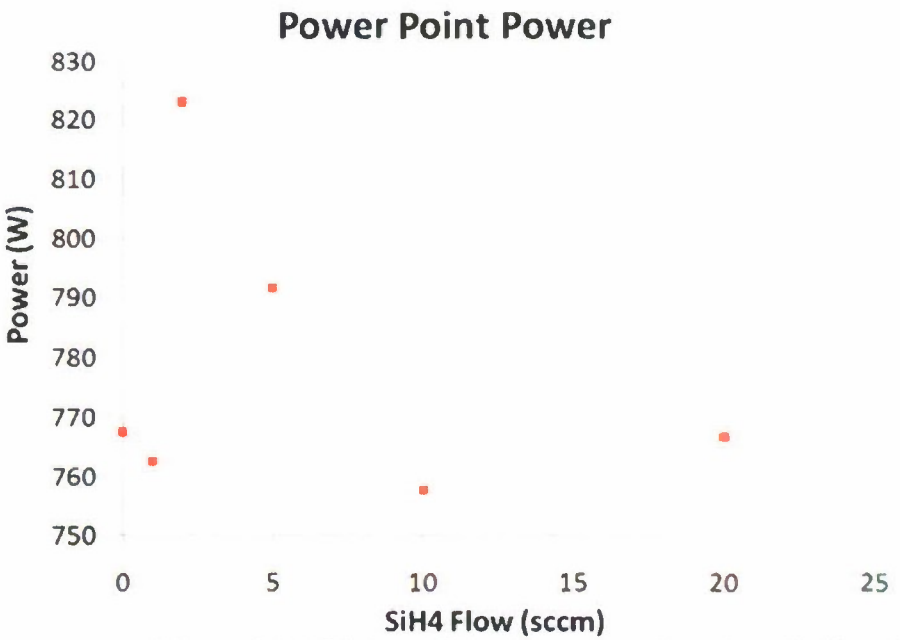


Figure A.2.20 Power Point Power as a function of silane flow with an acetylene flow of 0.1 sccm.

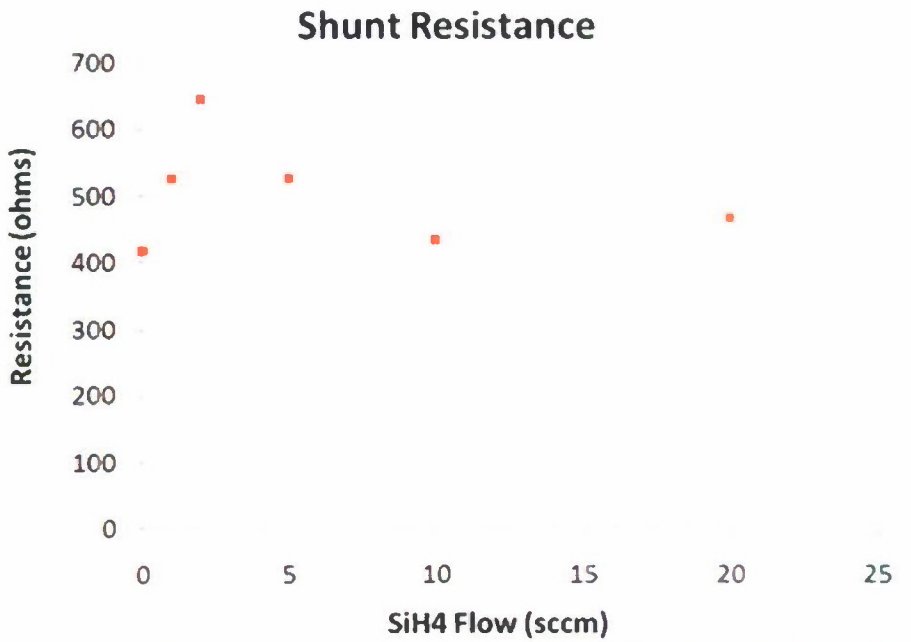


Figure A.2.21 Shunt resistance as a function of silane flow with an acetylene flow of 0.1 sccm.

In addition to an increase in voltage, the shunt resistance also initially increased with silane flow and then decreased as shown in figure 4. The initial increase in shunt resistance may be due to the defects in the recombination layer causing the layer to have a high lateral resistance, which makes it difficult for shunt paths in the top cell to find a low resistance route to shunt paths in the bottom cell. After increasing the silane flow past 2 sccm the shunt resistance decreases. This may be due to the reduction in defect states in the recombination layer caused by an increase in the ratio of silane to acetylene. This indicates that there is an optimum recombination layer thickness.

This data shows that use of a silicon carbide alloy deposited using acetylene and silane has the ability to produce a very defective layer, which promotes effective recombination between the two PIN diodes of a tandem photovoltaic module. These results are similar to earlier results using sputtered TiN as a recombination layer. The data from the experiments performed last month indicated a maximum in the open circuit voltage C2H2 flow of 0.1 sccm and SiH4 flows of 2 sccm.

It was found that this method works well giving open circuit voltages of up to 21.4 volts, however there were repeatability problems caused by buildup of deposition on the walls of the deposition zone. This method is more sensitive to deposition buildup because of the high voltages required at the low gas flows and pressures used in this process.

**Front side roller**

A test was set up so that a physical contact was made to the device side of the web during the silicon deposition. A roller assembly was positioned in the web path so that it contacted the web between the top and bottom layers of the tandem solar device. No external gases or reaction were present at this roller.
It is believed that the ambient gases surrounding the roller cause a surface contaminant that collects of the roller's surface which then transfers to the web.

The results for this test were comparable to that of the TiN layer. These results were reproduced. Being of simple design and utility, it shows great promise of implementation. The concern we have for this process is that the environment contains a large number of small particles. These particles can collect in the bearings of the roller and cause them to fail. When the roller ceases motion it would then scratch the device material damaging the electronic properties of the resulting solar module.

### A.3) Design system for in-line deposition of recombination layer and install in Si system

The current set up, as describe in section A.3.2 above, using a DC plasma zone with acetylene in line with the PV deposition process is satisfactory. Alterations to include this system in the primary production system would be minor and only for accessibility by the operators.

Additionally, a front side roller assembly can be easily substituted for the plasma zone.

### A.4) Develop optimum operational parameters for recombination layer

Over the course of this study a series of different deposition techniques and materials were studied to determine both their ability to reliably form an effective tunnel-recombination junction and ability to adapt them to PowerFilm's existing process equipment. Table A.4.1 shows the different tunnel-recombination junction surface treatments, the materials deposited, the final open circuit voltages, and the tool the deposition was performed in.

| Surface Treatment | Material | Open Circuit Voltage | Deposition Tool |
|---|---|---|---|
| None | Base Material | 19.6 | Insitu |
| None | Decrease I2 H2:SiH4 dilution ratio | 20.2 | Insitu |
| DC-PECVD | Amorphous Silicon | 21.5 | Insitu |
| DC-PECVD | Amorphous Silicon-Carbide | 21.4 | Insitu |
| Front Surface Roller | No Deposition | 22.1 | Insitu |
| Hot-Wire CVD | Amorphous Silicon | 21 | Insitu |
| DC Sputtering | Titanium Nitride | 22 | Metal Machine 2 |

| | | | |
|---|---|---|---|
| RF Oxygen Plasma | Silicon Dioxide | 20.1 | Oxygen Etch |

Table A.4.1 Open circuit voltage comparison for various surface treatments.

Initially, Power Film's base material had an open circuit voltage of about 19.6V.

Three surface treatments were performed requiring depositing the bottom junction of the solar cell, then removing the material from the silicon deposition system, placing it in a second system for tunnel-recombination layer deposition, and then placing it back in the silicon chamber to finish the silicon deposition. The first treatment was the addition of a DC sputtered titanium nitride layer deposited in Power Film's Metal Machine 2. This material increased the open circuit voltage up to 22V, however it had repeatability problems and sputtering is not easily compatible with our current deposition systems. The third surface treatment was an RF oxygen plasma treatment in Power Film's Oxygen Etch system. This surface treatment did not demonstrate an increase in open circuit voltage, so it was dismissed.

Two in-situ surface treatments were performed. The first was deposition of amorphous silicon using hot-wire chemical vapor deposition. This method was able to deposit a tunnel-recombination junction that increased the open circuit voltage to 21V, however it had many problems. The largest problem was the non-uniformity of deposition rate in the cross-web direction due to the filament sagging. Many experiments were performed to overcome the sagging including intermediate supports, wrapping the filament around a ceramic rod, tensioning the filament, and using a different material that is more rigid. It was determined that this process was not robust enough to achieve repeatable cross-web uniformity and filament lifetime. The second in-situ method was using DC-PECVD to deposit a layer of amorphous silicon or amorphous silicon carbide. Amorphous silicon deposited with this method yielded an open circuit voltage of 21.5V, while the amorphous silicon carbide yielded an open circuit voltage of 21.4V. This method works on short runs, however has some repeatability problems caused by buildup of deposition on the walls of the deposition zone. This method is more sensitive to deposition buildup than the RF-PECVD used to deposit the other silicon layers because of the high voltages required at the low gas flows and pressures used in this process. The second surface treatment was performed by simply adding a roller between the P1 and N2 deposition zones that the deposition surface of the web comes into contact with. Contact with this roller changes the surface of the P1 layer enough that when the growth of the N2 layer is initiated more defects are created. The open circuit voltage achieved using this surface treatment was 22.1V. Preventative maintenance is very important when using this approach because if a bearing is not turning freely, then the surface of the web will be scratched and create shunts in the material.

To incorporate the tunnel-recombination junction into future machines, the front surface roller approach will be used. It has the advantage of not requiring any extra source gases or electronic equipment and also yielded the highest open circuit voltages. If a preventative maintenance schedule is followed this approach should work very well.

## B. Long-term Stability

### B.1) Design set of experiments and fabricate samples to evaluate impact of variables including spacing and electrode heating on device stability

Prolonged light soaking of a-Si has the effect of trapping carriers to create metastable states which reduce mobility and therefore efficiency. These metastable states also empty at a rate determined by density and temperature, so that equilibrium is reached. We want that equilibrium to be as low as possible so that the device stabilizes at an efficiency which is as high as possible.

Power Film studied the potential for improving long term stability in our photovoltaic devices by looking at a number of deposition parameters in the first intrinsic layer, I1-layer. These included; evaluating the impact of pressure, temperature, RF power level, silane flow rates, and hydrogen dilution. The range these variables are maintained with in conditions which are compatible with all other operational constraints.

Our standard method for evaluating stability is to use a full 12 cell module of single junction material of the thickness and deposition properties under study. Light soaking is done for 30 days outdoors under open circuit conditions. Open circuit conditions provide a higher rate of trapping and defect creation and a higher equilibrium level than would be seen under normal operating conditions. Normally the equilibrium level of defects is reached asymptotically over a long time, but we have found that 30 days under open circuit gives a good approximation of the equilibrium state which would be reached if the module were operating at its power point.

Operating with the above parameters; higher I1 box pressures has been shown to produce better cross-web uniformity of the silicon deposition. The higher pressure improves the uniformity significantly, keeping 5% thickness tolerance to within 1" of the web edge. PowerFilm then identified the proper subset, with variations on flows, RF powers, and antenna spacing which give improved stability against light soaking. The concern with operating at higher pressures, even though it may produce more uniform film thickness, is that it can lead to the generation of dust particles in the process. This dust can adhere to the web during processing and cause electrical shunting of the material. These Initial test data indicated that the higher pressure run parameters did not cause issues with dust.

These module samples were given a 30 day light soaking exposure on an out doors test platform. Data was taken from these devices which were prepared with a set of parameters that would enable us to quickly isolate important variables. Fill factor (FF) is the key parameter affected by light soaking with a FF remaining higher over time indicating less degradation. In the past, we had reduced thickness of the I1- layer in attempts to improve stability and revisited this parameter to insure that the process change resulted in stability at least as good or better as the prior conditions. Figure B.1.1 shows samples from the old and new conditions. It shows no change in the stability dependence on the pressure parameter and that the new condition, Series 2, falls on the

same thickness trend line as the lower pressure conditions, Log(series2). This confirms that pressure, though important for uniformity, is not as significant for long term stability.

The results of the 30 days testing, the film thickness and deposition conditions were analyzed for potential modifications to reduce the level of degradation. Based on these efforts, I1 layer deposition zone temperature and hydrogen dilution were down selected as variables to focus on. Other variables, such as antenna spacing and RF power levels did not show that they had a significant impact on long tern stability.

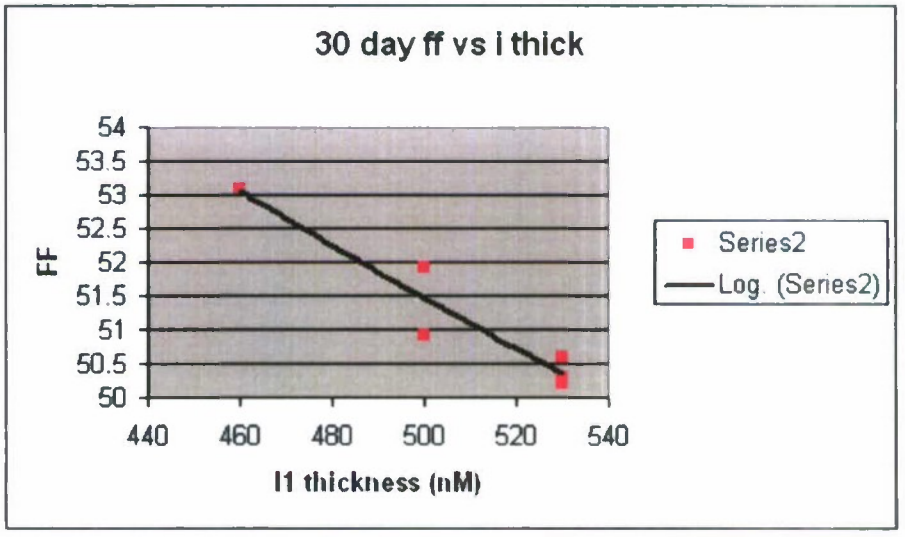


Figure B.1.1 Showing the 30 day fill factor, FF, as a function of I layer thickness.

A series of runs were performed with increasing pressures in steps from 500 mtorr to 1000mtorr and powers from 200W to 400W while varying the H2/SiH4 ratios from 3 to 10 and varying total gas flows over a range of 700 SCCM to 2500 SCCM. In evaluating this broad range of parameter space, conditions were identified which retain our current deposition rate and uniformity while moving the H2/SiH4 ratio up to 10. Small dot samples were tested and have validated device operation under those conditions and full module samples were produce for long term study.

Out of these, sample prepared with a H2/SiH4 ratio of 5 and standard power showed extremely good stability, though they had a lower current because the thinner I -layer. The samples at 400W showed improved stability of Fill Factor as opposed to our standard material. These higher RF power samples did have a lower initial performance than the standard power samples, so that in the end, the final performance was equivalent.

The higher H2 dilution showed better performance, but the question remained whether it was the dilution or was it the film thickness the important factor. A test was run with high dilution and at a slower speeds to maintain a constant film thickness so that the important factor could be sorted out. These samples were light soaked for three weeks. Samples with high H2 dilution and slow web speeds, providing the standard 500 nm I-layer thickness, show no improvement over the standard material. It was concluded that the improved stability of prior samples was due to the thin I layer. This left higher

deposition temperature and reduced thickness as the two successful mechanisms for improving stability of the I1 junction.

Our final tests were combining these two effects. The higher temperature reduces band gap and allows for more light to be collected for an equivalent thickness, so moving to 190C should allow us to reduce the I-layer thickness. However, higher temperatures create higher stress in the deposited films. These stresses may be accommodated by using lower CTE polyimide or by adding a stress balaneing back layer. A series of samples were prepared at a temp of 290C and a variety of thicknesses. Thickness variation was accomplished by increasing H2 flow while keeping silane flow and power constant. We found, that with this combination, we were able to reduce the I1 layer thickness by 100nm (about 20%) with negligible loss of current as compared to our standard thickness at 275C . The light induced degradation of fill factor was reduced by 25% in going to these new conditions.

**B.2) Perform tests including lifetime testing (light soaking and damp heat) on samples as appropriate. Repeat with modified operating parameters as indicated by results.**

Multiple full production runs on different silicon deposition machines were produced using the chosen subset of variables, including temperature and I1-layer thickness.

Thirty day outdoor testing was performed on these samples to evaluate the stability impact across the web, down the web, and from machine to machine. This evaluation found that the life time improvements held throughout the length of the deposition and transfers from machine to machine.

## C. Carbon Doping

### C.1) Identify appropriate carbon source gas

PowerFilm has identified acetylene as the carbon source to use. To minimize the impurity contamination from the source gas, acetylene in Dimethylformamide was used.

### C.2) Obtain appropriate source gas and equipment and install on existing PV deposition machines

Two key elements of this work have been delivered and installed on one of PowerFilm's silicon deposition system in February 2010. These are the acetylene gas source and mass flow controller, and a Keithly model 617 electrometer. This instrument will be used to measure the activation energies of the carbon-silicon films.

The aeetylene gas source and equipment was acquired and installed. Ultimately it was found that a lower coneentration of acetylene was required and a switch was made to using acetylene diluted to 5% in helium.

## C.3) Identify operating parameters to deposit Si-C firms

An initial series of silicon/carbon film depositions were made on specular metallized web material. The depositions were made with varying amounts of acetylene (C2H2) flow 0, 10, 20, and 30% C2H2 with these percentages representing percent of total silane flow. These films were deposited at a web speed of 3 inches per minute, which we would expect to be around 100nm of deposition. Surface Photo Voltage measurements of these films demonstrated that the material properties changed with addition of the acetylene, figure C.3.1 below.

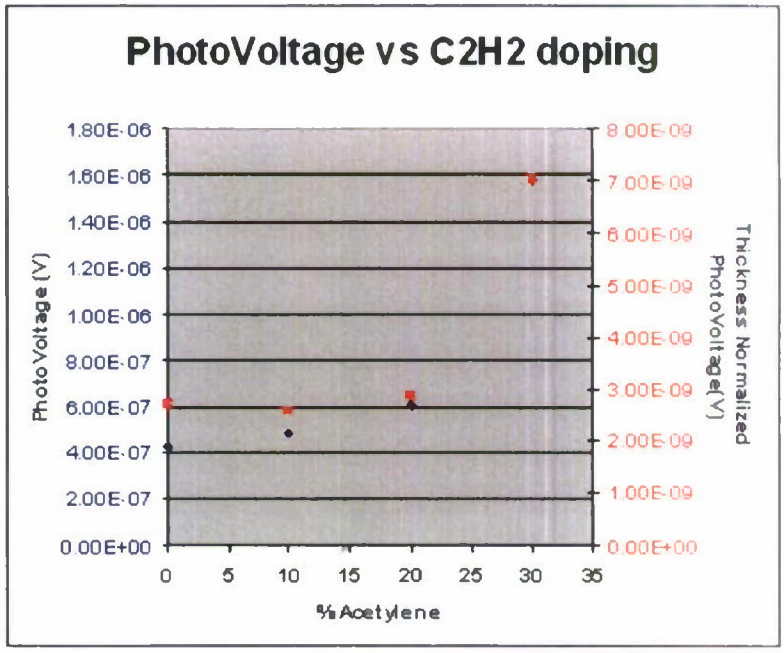


Figure C.3.1 Surface photo-voltage measurements on silicon carbon film as a function of percent acetylene addition.

Thickness measurements were made on these films using a step profilometer allowing for deposition rate to be calculated for each condition as shown in Figure C.3.2.

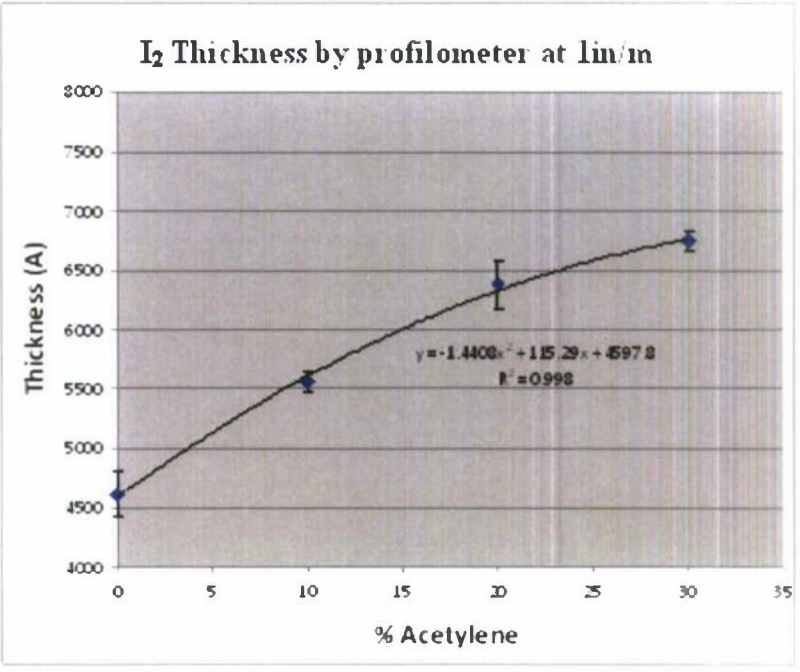


Figure C.3.2 Film thickness as a function of percent acetylene.

Measuring the reflection spectra and using the relationship;

$$2nd = (m + {}^{1}/_{2})\lambda$$

for minima's in the spectrum, where wavelength ($\lambda$), the film thickness is d, and minima order m, where n is the refractive index was calculated, figure C.3.3. The index shifted as expected for increasing carbon content in the film. At the high end of carbon content, the index of refraction is approached that of report values for silicon carbide of 2.55.

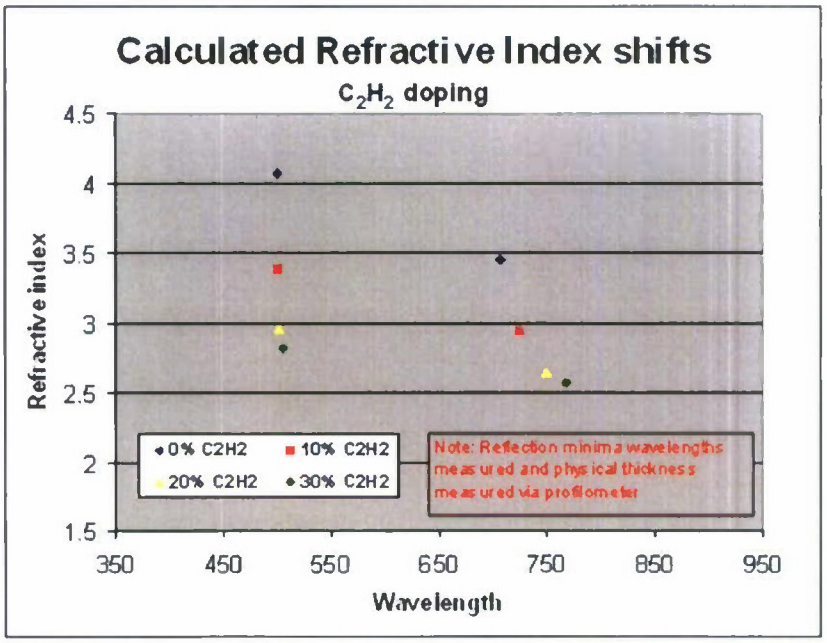


Figure C.3.3 The index of refraction of the silicon-carbon films using different spectral minima, indicating the index as a function of wavelength of light for varying carbon content.

A Keithly model 617 electrometer was used to measure activation energy of carriers and light-dark conductivity of samples of silicon carbide (a-SiC) prepared on insulating substrates, see data in Table C.3.1.

| Sample | Light Conductivity | Dark Conductivity | Light/Dark Ratio |
|---|---|---|---|
| 10% C2H2 | 2.70E-10 | 3.2e-11 | 8.44 |
| 20% C2H2 | 6.5e-11 | 3.5e-11 | 1.86 |
| 30% C2H2 | 1.90e-10 | 4.8e-11 | 3.96 |

Table C.3.1 Properties of carbon doped silicon films.

The Light/Dark ratio indicated that the defect generated charge carriers are dominating the electrical characteristics of the film.

The activation energy was measured for the 20% sample. The natural log of the current (Ln(I)) versus reciprocal temperature (1/T) is shown. From the slope of the fitted line the

activation energy was found to be 0.76eV. This value is in the range of what is expected for this material, Table C.3.2.

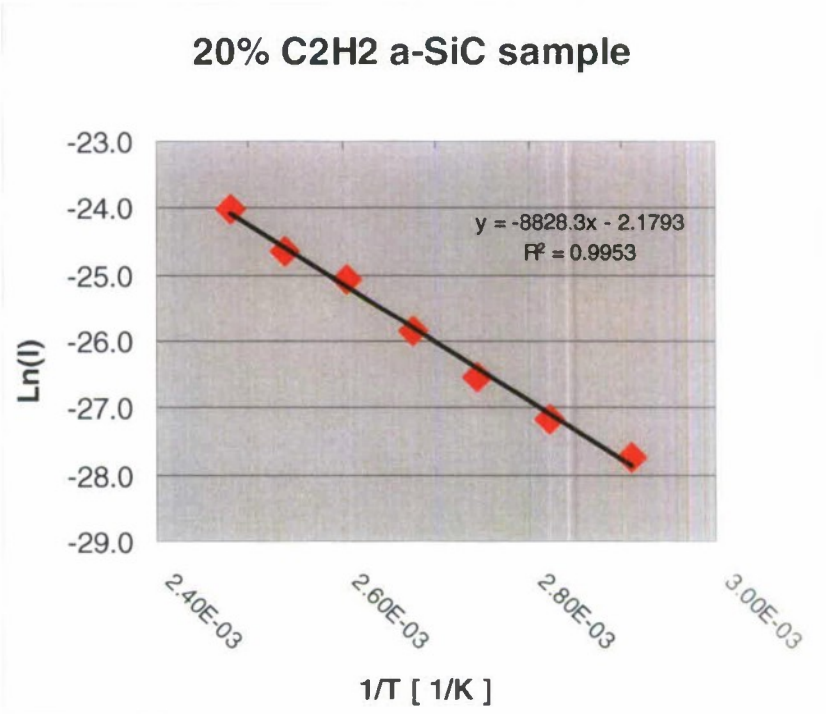


Table C.3.2 the natural log of the current (Ln(I)) versus reciprocal temperature (1/T) is shown.

The Si-C material was then substituted for the intrinsic amorphous silicon. None of the Si-C samples (10%, 20%, & 30%) created a photovoltaic junction, leaving us to concluded that the Si-C layer is highly defective and does not allow for charge separation.

Si-C films were produced at lower carbon flow rates of 3% and 6%. Thickness and reflectance measurements of the films were measured and the refractive index was calculated. See figure C.3.4.

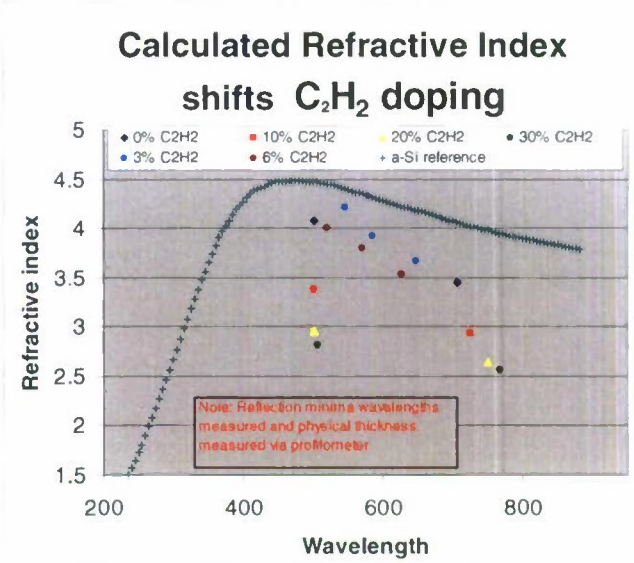


Figure C.3.4. The 3% and 6% data points have been added to a previously seen graph. The refractive index continues the trend of higher index with less carbon.

Using 0%, 1%, and 3% Acetylene flow PV single junction material was made. Both the 0% and 1% Acetylene flows produced junctions with fill factors between 49% & 52%, see figure C.3.5. The 3% sample was completely resistive indicating an upper boundary for the acetylene flow.

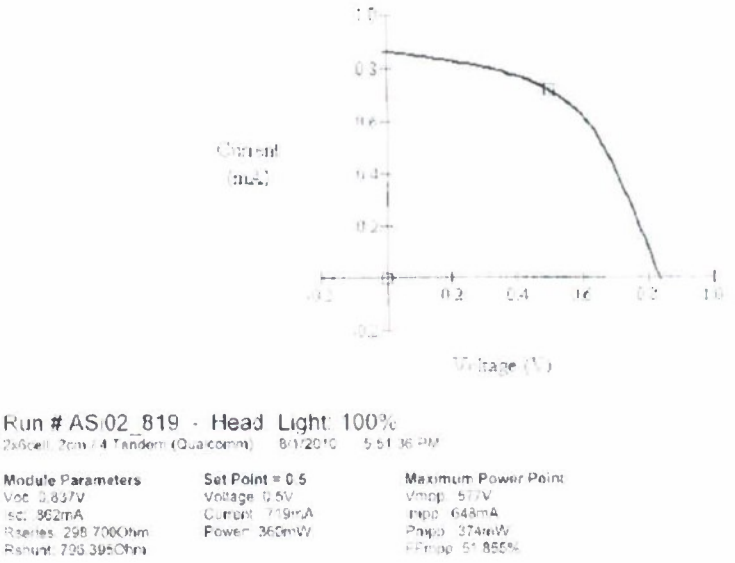


Figure C.3.5 I-V curve of a carbon doped amorphous silicon solar cell.

A series of single junction material were made using the 10sccm MFC with varying amounts of acetylene at 0%, 0.48%, 0.85%, 1.2%, and 2.4% of the Silane flow for the intrinsic layer. Dot samples were made and measured the values appearing consistent, figure C.3.6.

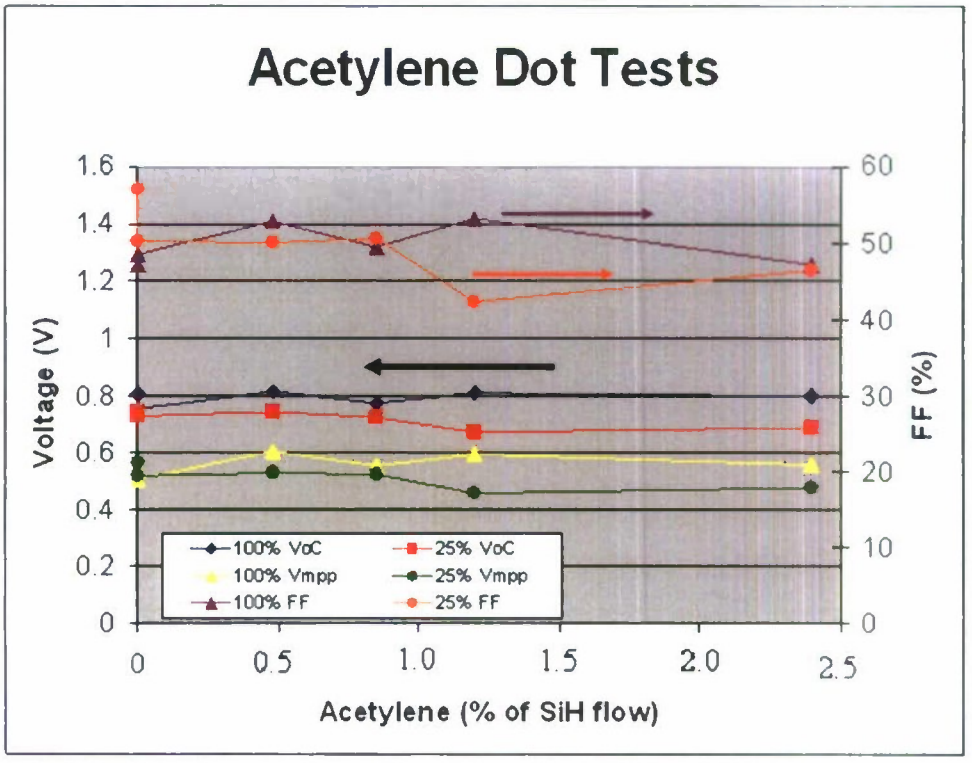


Figure C.3.6 Measured parameters for carbon doped amorphous silicon solar cell.

SEM images were taken of the layers with and without acetylene doping. Visual inspection of the grain structure shows a variation in islanding with acetylene. This indicates a structural change with the addition of the acetylene, Figure C.3.7.

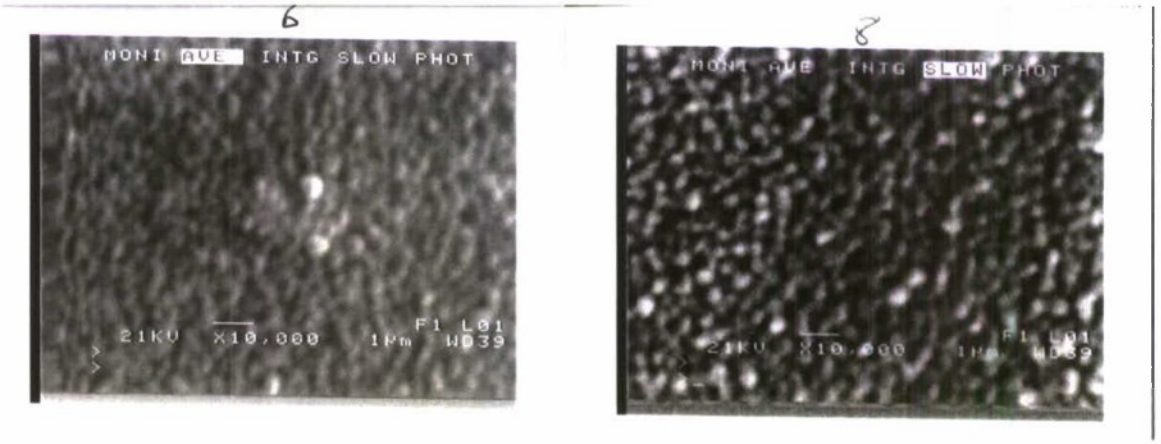


Figure C.3.7 Sample 6 is 0% acetylene and Sample 8 is 2.4% acetylene.

Tandem junction PV material was deposited with varying amounts of acetylene (C2H2) doping from 0 to 1.5% of the I2 layer of a tandem junction. Both the peak Voc and the average Voc for each flow trend higher with Acetylene flow. Also an upper limit of Acetylene flow of 2.5secm, or 6.25%, was identified as point at which above this, devices

fail and no longer give PV electrical response. Likewise, Fill Factor, and maximum power point were plotted against the Acetylene flow, figures C.3.8-10. The fill factor and Power at max power-point of each sample also increase with Acetylene flow up to about 1 sccm.

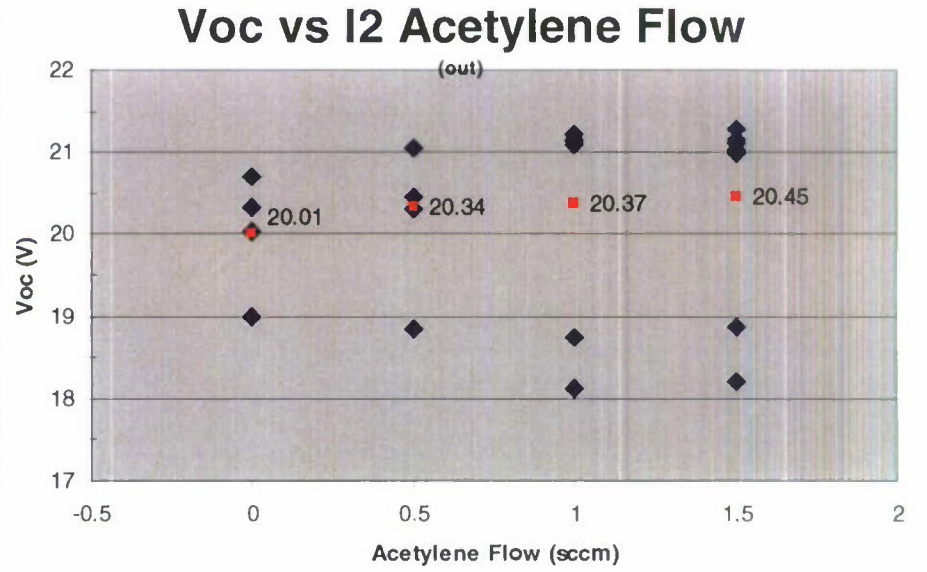


Figure C.3.8 Open circuit voltage, Voc, plotted against the Acetylene flow. Each sample measured is represented by a blue diamond on the graph; the average for each flow set point is displayed as a red square.

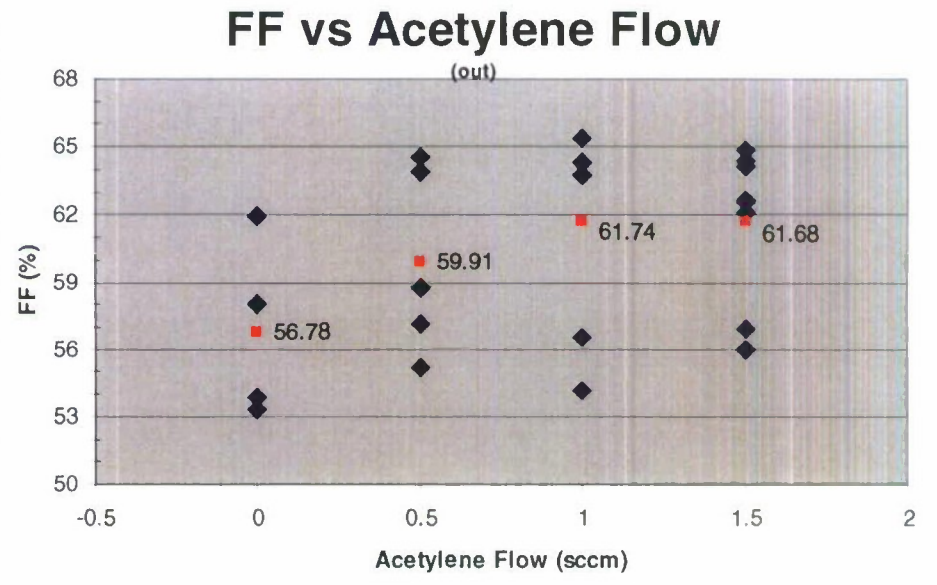


Figure C.3.9 Fill Factor, ff, plotted against the Acetylene flow.

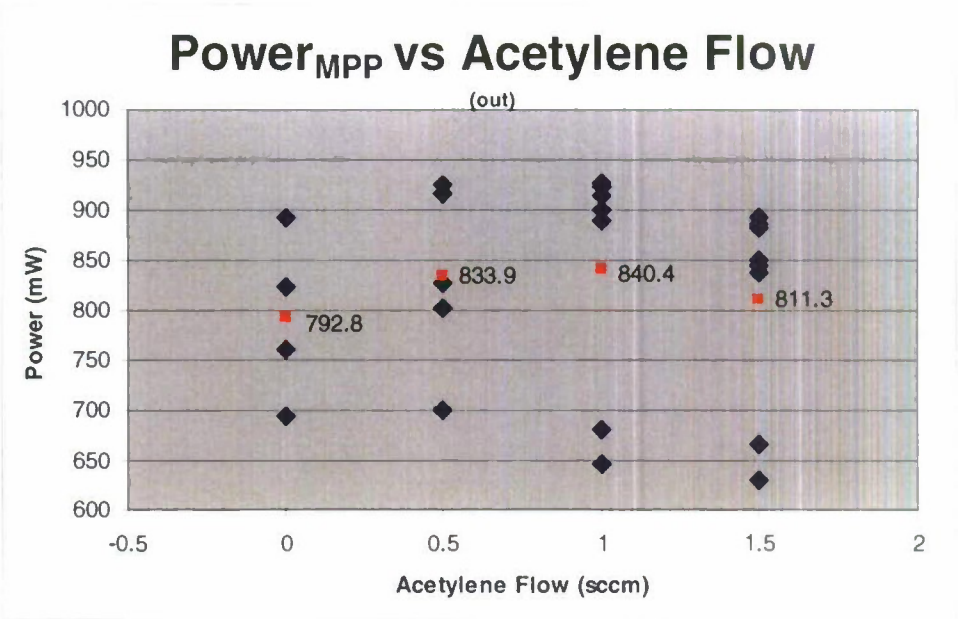


Figure C.2.10 Maximum power point power, MPP, plotted against the Acetylene flow.

Samples with and with out carbon doping were sent to an external application lab for Spectroscopic Ellipsometry to find the refractive index and film thicknesses. The ellipsometry data (n,k), for the individual $I_2$ layers from those cells, shows a shifting of the absorption curve up to 35nm towards the blue end of the visible spectrum as compared to standard amorphous silicon films. At higher doping levels, the spectrums returned to the standard index which may be indication that non-substitution carbon doping (interstitial) is taking place at higher levels of acetylene flows. This data indicated that the optimum results are achieved near the 0.5% doping level (absorption blue shift of 35nm). Figures C.3.11 and C.3.12

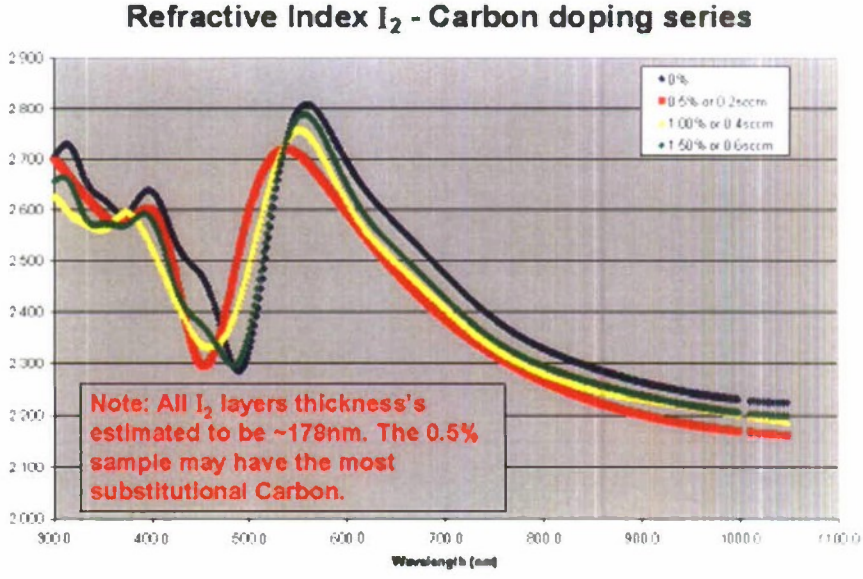


Figure C.3.11 Refractive index of carbon doped amorphous silicon as measured with ellipsometery. (0% is Power Film's standard material.)

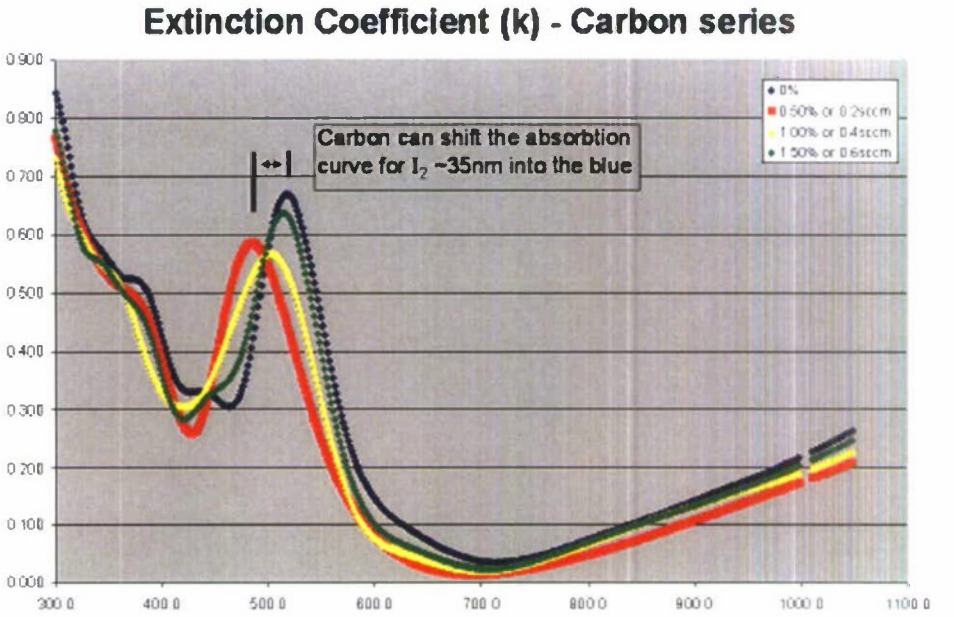


Figure C.3.12 Extinction coefficient of carbon doped amorphous silicon as measured with ellipsometry. (0% is Power Film's standard material.)

A series of samples were made using doping concentrations centered around 0.5%. The doping concentrations achieved were 0.43%, 0.5%, 0.59%. The main effect, of the carbon doping of I2, appears to be an increase in the Voc. Figure C.3.13

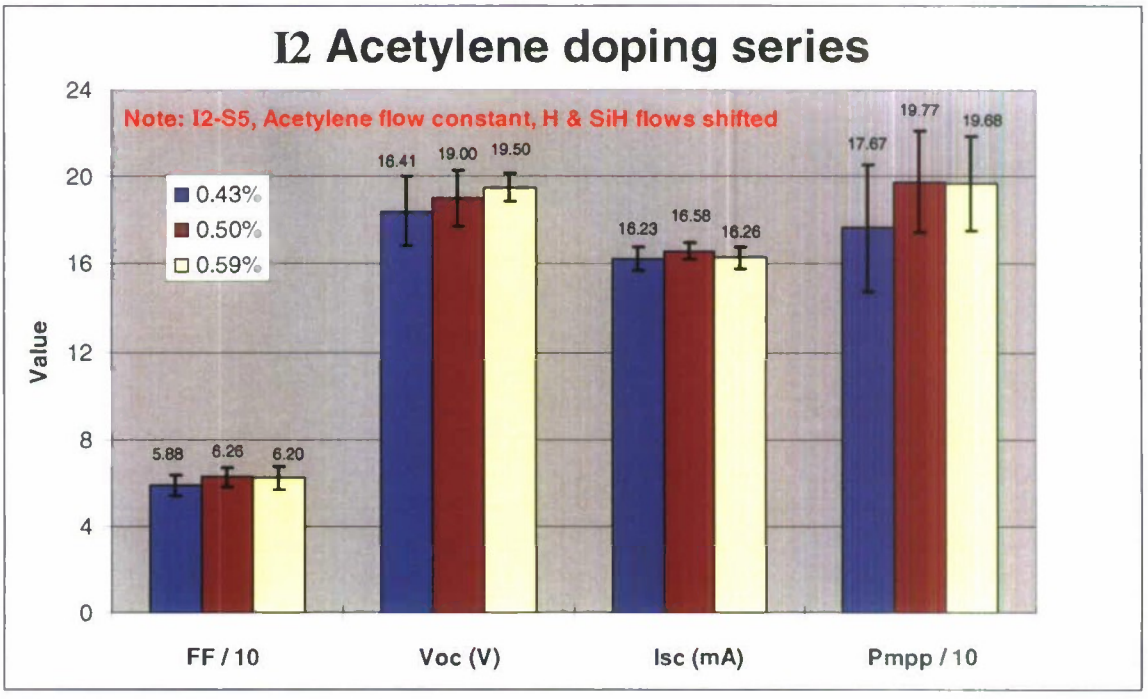

Figure C.3.13 IV curve test of PV modules with carbon doping. Note: the fill factor (FF) and power at max power point (Pmpp) are divided by a factor of 10 for displace purposes.

To increase resolution and repeatability of the carbon doping concentration, the source bottle of acetylene was replaced with one of 95% He and 5% C2H2. This will allow acetylene for flows from 0 .05sccm to 1 sccm.

A study of the thickness for the I2 layers was completed. This was to verify that the I2 thickness is set to maximize the power created by the tandem cell. If the I2 layer is too thin, too few carriers are created in the I2 layer and power is lost in the I1 layer. If the I2 layer is too thick, too few carries are created in the I1 layer and power is lost in the I2 layer. So in order to maximize performance, the tandem cells must be balanced with the power they generate.

Variations of the I2 thickness was achieved by adjusting the RF power to the I2 box. The acetylene flow was 0.5sccm and it was kept constant at a 80:1 (SiH4:C2H2) ratio for all of the doped samples. Figure C.3.14

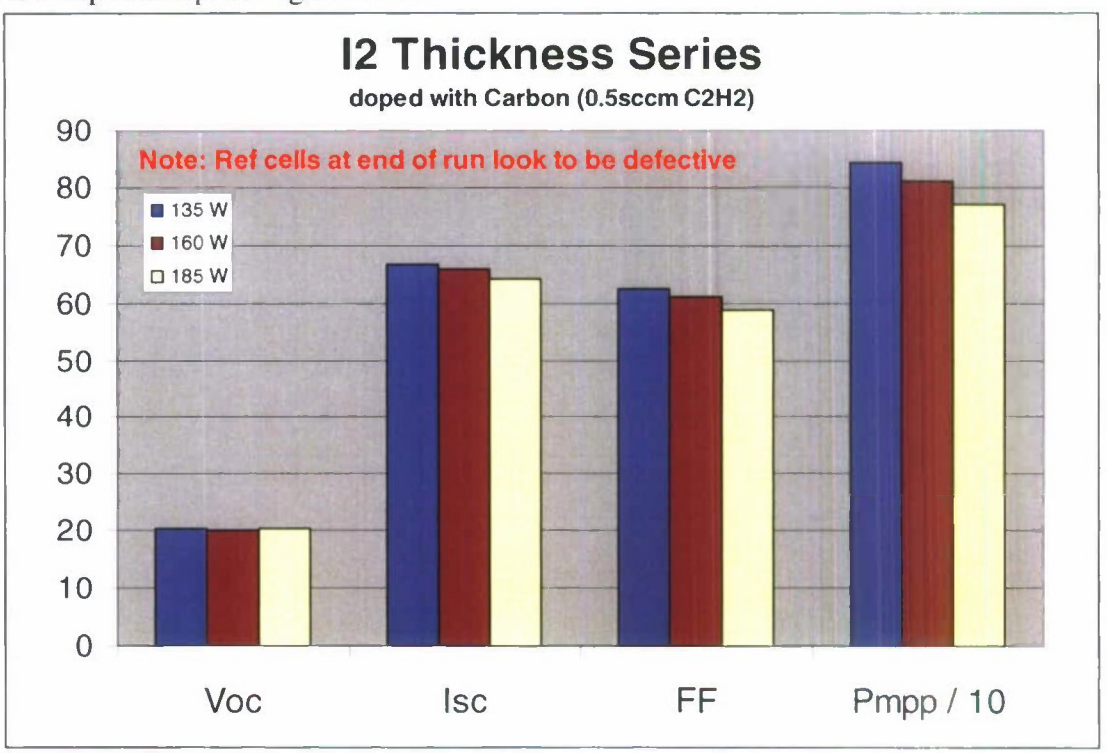


Figure C.3.14 The graph below shows the electrical results for Voc, Isc, FF, and Pmpp. There trend is towards lower RF power or thinner layers of carbon doped I2.

We were able to successfully incorporate Carbon into the amorphous I2 layer, and found that acetylene works as an efficient dopant. We found that the carbon caused a shift in the measured refractive index via spectroscopic ellipsometry. The bandgap was blue shifted which would allow more red light to reach the I1 layer. The carbon doping

improved all aspects of the PV modules performance including power output. We saw approximately a 5% gain in module output by incorporating carbon into the 12 layer. This could lead to increased power per unit area and lower Dollars/Watt.

### C.4) Build and test PV devices

As stated in PowerFilm Inc.'s proposal, they will produce and deliver 10 prototype lightweight, foldable PV units suitable for use with BB2590/BB390 chargers or other similar applications, along with technical data from the program.

The resulting PV modules had outdoor, natural sunlight, performance curves with fill factors near 65% and power point voltage of over 16 volts, power point current of over 56mA, giving a power point power of nearly 900mW.

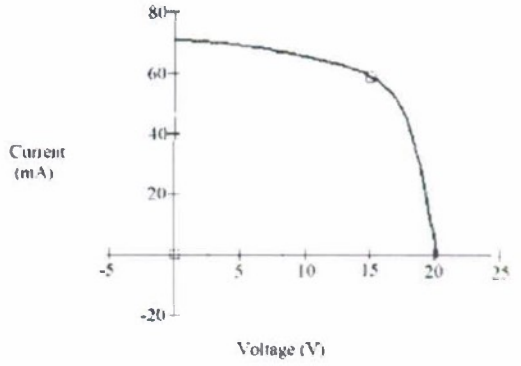


Light Out%

N/A 2/8/2011 10:39:40 AM Ref Cell 2.65mA Stc Ref Cell 3.14mA

| Module Parameters | Set Point > 15.0 | Maximum Power Point |
|---|---|---|
| Voc 20.75v | Voltage 15.0V | Vmpp 16.042v |
| Isc 70.838mA | Current 59.153mA | Impp 56.533mA |
| Rseries 4.734Ohm | Power 887.445mW | Pmpp 903.691mW |
| Rshunt 3184.682Ohm | Adj Current 57.930mA | FF 62.225% |
| Adj Isc 68.147mA | Adj Power 868.450mW | |

Figure C.4.1 IV curve representing the deliverable material.

### C.5) Fabricate Deliverables

Deliverables will be shipped to:

U.S. Army Soldier Systems Center – Natick
Attn: Steven Tucker
Kansas Street
Natick, MA 01760-5000
MARK FOR: W911QY-10-C-0019